Glucosamine HCl-based solid dispersions to enhance the biopharmaceutical properties of acyclovir.

Darshan R. Telange[a], Snehal B. Bhagat[a], Arun T. Patil[a], Milind J. Umekar[a], Anil M. Pethe[b], Nishikant A. Raut[c], Vivek S. Dave[4*]

[a]Rajarshri Shahu College of Pharmacy, Malvihir, Buldhana, Maharashtra, India
[b]Shobhaben Pratapbhai Patel School of Pharmacy & Technology Management, SVKM'S NMIMS, V. L. Mehta Road, Vile Parle (West) Mumbai, Maharashtra, India
[c]University Department of Pharmaceutical Sciences, R. T. M. Nagpur University, Maharashtra, Nagpur
[d]St. John Fisher College, Wegmans School of Pharmacy, Rochester, NY, USA

Received: June 5, 2019*; Accepted:* August 6, 2019

Original Article

ABSTRACT

The objective of the work presented here was to assess the feasibility of using glucosamine HCl as a solid-dispersion (SD) carrier to enhance the biopharmaceutical properties of a BCS class III/IV drug, acyclovir (ACV). The solid-dispersions of acyclovir and glucosamine HCl were prepared by an ethanol-based solvent evaporation method. The prepared formulations characterized by photomicroscopy, scanning electron microscopy (SEM), differential scanning calorimetry (DSC), Fourier transforms infrared spectrophotometry (FTIR), powder x-ray diffractometry (PXRD) and drug content analysis. The functional characterization of ACV-SD was performed by aqueous solubility evaluation, dissolution studies, fasted *versus* fed state dissolution comparison, ex vivo permeability, and stability studies. Photomicroscopy and SEM analysis showed different surface morphologies for pure ACV, glucosamine HCl and ACV-SD. The physical-chemical characterization studies supported the formation of ACV-SD. A 12-fold enhancement in the aqueous solubility of ACV was observed in the prepared solid dispersions, compared to pure ACV. Results from *in vitro* dissolution demonstrated a significant increase in the rate and extent of ACV dissolution from the prepared ACV-SD formulations, compared to pure ACV. The rate and extent of ACV permeability across everted rat intestinal membrane were also found to be significantly increased in the ACV-SD formulations. Under fed conditions, the rate and extent of the *in vitro* dissolution of ACV from the formulation was appreciably greater compared to fasted conditions. Overall, the results from the study suggest the feasibility of utilizing glucosamine HCl as a solid dispersion carrier/excipient for enhancement of biopharmaceutical properties of acyclovir, and similar drugs with low solubility/permeability characteristics.

KEY WORDS: Acyclovir, ACL, glucosamine HCl, solid dispersion, solubility, permeability, excipients

INTRODUCTION

Modern drug discovery techniques, which include high throughput screening and combinatorial chemistry, have generated new molecules with solubility characteristics that result in lower and inconsistent oral bioavailability (1). Over half of all newly discovered drugs appears to fall into biopharmaceutics classification system's (BCS) class II (↓ solubility, ↑ permeability), Class III (↑ solubility, ↓ permeability) or class IV (↓ solubility, ↓ permeability) (2). These drugs exhibit dissolution and/or permeation rate-limited absorption. For these drugs, enhancement of dissolution rate and/or permeability is vital to attain suitable blood concentration to achieve optimal bioavailability for therapeutic effect (3-5). Thus, for a formulation development team, there is a consistent and well-justified need to explore

*Corresponding address: Vivek S. Dave, St. John Fisher College, Wegmans School of Pharmacy, Rochester, NY, 14534, Tel: 1-585-385-5297, Fax: 1-585-385-5295, E-mail: vdave@sjfc.edu

approaches that improve the dissolution and/or permeability characteristics of such drugs.

Among the popular approaches explored in the past decade to achieve this goal include the micronization of drugs, formulation of drugs into liposomes, microspheres, microemulsions, inclusion complexes, nanoparticles, self-micro emulsifying drug delivery systems, solid dispersions, and other non-traditional drug delivery systems (6-14). Among these, formulating drugs into solid dispersions to improve their biopharmaceutical properties has gained widespread traction and acceptance. Solid dispersions are typically formed by uniformly dispersing one, or more, APIs into a hydrophilic matrix carrier using thermal, mechanical, co-solubilizing or a combination of one or more similar techniques (15, 16). Within a solid dispersion, the solubility and permeability of the API is reported to be improved by, a) the reduction of particle size of the drug to sub-micron or smaller, allowing increased surface area for dissolution, b) the alteration of a crystalline drug to a high energy amorphous state, and c) increasing wettability of the drug particles in an aqueous environment (16, 17). The development of a successful solid dispersion often depends on the choice of the carrier material, as well as, the processing method.

Acyclovir is an antiviral drug, commonly prescribed for the treatment of infections caused by the herpes simplex viruses (HSV-1 and HSV-2) and the varicella-zoster virus. Depending on the available strength of the tablets, acyclovir has been classified as either a BCS class III or a class IV drug (18). Upon oral administration, acyclovir exhibits low oral bioavailability (~15-30%) (19). The low bioavailability of acyclovir is attributed to its poor aqueous solubility, as well as, low permeability (20-23). Therefore, acyclovir was selected as a model drug for this study with the objective to improve its dissolution and permeability characteristics.

Glucosamine is a naturally occurring amino-monosaccharide obtained from glucosamine-6-phosphate *via* a hexosamine biosynthetic pathway. Structurally, it is a 2-amino-2-deoxy-β-D-glucopyranose with the molecular formula ($C_6H_{13}NO_5$). It is a non-toxic and a highly water-soluble (320 mg/mL) compound (24, 25). Among its salts, that is hydrochloride (HCl), sulfate and N-acetyl, the HCl salt is pharmaceutically acceptable due to its high aqueous solubility and physical stability. The hydrophilic nature of glucosamine HCl is reported to improve drugs with poor aqueous solubility and permeability by improving particle wettability in an aqueous environment (26). Despite its potential drug delivery optimizing benefits, the usage and applications of glucosamine HCl as a carrier in the designing of novel drug delivery systems remains largely unexplored. In recent years, only a few publications originating from the group of Al-Hamidi *et. al.* have reported the potential for using glucosamine HCl as a solid dispersion carrier (26, 27). While useful and informative, these studies can be considered insufficient in terms of material characterization and functional analysis of the formulations.

Therefore this study describes a systematic and comprehensive feasibility analysis of using glucosamine HCl as a solid dispersion carrier for improving the dissolution and/or permeability characteristics of acyclovir. For the study, acyclovir solid dispersion formulations (ACV-SD) with increasing ratios of glucosamine HCl were prepared using an ethanol-based, solvent-evaporation method. The prepared ACV-SD were subjected to physical-chemical characterization with scanning electron microscopy, particle size and zeta potential analysis, thermal analysis, Fourier transforms infrared spectroscopy, powder x-ray diffractometry, aqueous solubility, and drug content analysis. The ACV-SD were further characterized for their functionality via dissolution and permeability studies, and fasted- and fed- state dissolution studies. Finally, the influence of controlled-storage conditions on the functional attributes of ACV-SD was evaluated by conducting a preliminary stability study for a period of six months.

MATERIALS AND METHODS

Materials

Acyclovir was obtained from Zim Laboratories Ltd., Nagpur, India. D (+) Glucosamine hydrochloride was

sourced from Sigma-Aldrich Corporation, St. Louis, MO, USA. Dichloromethane, ethanol, glacial acetic acid, soy lecithin, methanol, n-octanol, sodium hydroxide, and sodium taurocholate were acquired from Loba Chemical Pvt. Ltd., Mumbai, India. Calcium chloride, glucose, magnesium sulfate, potassium chloride, potassium dihydrogen phosphate, sodium chloride, and sodium bicarbonate were sourced from Merck Ltd. Mumbai, India. All other chemicals/solvents used were of analytical grade and used as received.

Preparation of acyclovir solid dispersion (ACV-SD)

Solid dispersions of acyclovir (ACV-SD) using glucosamine HCl as a carrier were prepared using different drug:carrier ratios (1:1, 1:2, 1:3, 1:4, and 1:5) according to the method previously described by Dhore *et. al.* (28). Briefly, acyclovir was weighed and dissolved in 10 mL ethanol. The ethanolic solution of acyclovir was then added to previously weighed glucosamine HCl in a mortar and blended thoroughly. The blending/trituration was continued until the ethanol was completely evaporated, forming a uniform dispersion. Complete evaporation of any residual ethanol was ensured by vacuum drying the samples at 40°C for 12 hours. The dried ACV-SD sample powders were stored in amber glass vials (flushed with nitrogen) at controlled room temperature (25°C) until needed. The composition of the prepared ACV-SD is shown in Table 1.

Table 1 Composition of the prepared acyclovir-glucosamine hydrochloride solid-dispersion formulations

FORMULATION	DRUG (MG)	CARRIER (MG)
ACV-SD1	100	100
ACV-SD2	100	150
ACV-SD3	100	200
ACV-SD4	100	250
ACV-SD5	100	300

Physical-chemical characterization of ACV-SD

Photomicroscopy and scanning electron microscopy (SEM)

The preliminary microscopic assessment of pure ACV, glucosamine HCl and the prepared ACV-SD was carried out using a digital microscope (Model: DM2500, Leica Microsystems, Germany). The samples for analysis were prepared by dispersing ~10 mg of either the drug, the carrier or the prepared formulation in 5 mL distilled water. A droplet from the uniformly mixed dispersion was then placed on a clean glass slide and observed under the microscope. The images of the samples were captured at different resolutions.

Additionally, individual samples were also examined for their surface characteristics using a scanning electron microscope (Model: Supra® 55, Carl Zeiss NTS Ltd., Germany). Briefly, the sample (~50g) was spread as a thin layer on a double-faced carbon tape, placed on the aluminum platform, which was then placed in the sample holder of the microscope. The sample was then coated with a thin layer of gold (~400 A°) using a sputter coater (Model: Supra® 55). The samples were scanned at an accelerating voltage of 10 kV, and the equipment-accompanied software (SmartSEM®, TV mode) was used to develop and record the images at different magnifications.

Particle size and zeta potential analysis

The particle size distribution of the prepared ACV-SD was performed on a Photon Cross Correlation Spectrometer (Model: NANOPHOX Sympatec, GmbH, Clausthal-Zellerfeld, Germany) with dynamic light scattering using a procedure reported by our laboratory earlier (29). The test samples were prepared by dispersing ACV-SD in deionized water. The analysis was performed at an operating sensitivity of 1 nm to 10 μm, and the particle count rate was optimized by the associated software.

The prepared ACV-SD were also analyzed for zeta potential using a Nano Particle Analyzer (Model: NanoPlusTM-2, Particulate system, Norcross, GA, USA). The analysis was carried out at a controlled temperature (25°C) and an operating range of -200 to +200 mV.

Thermal analysis

To evaluate any interactions between ACV and

glucosamine HCl, a differential scanning calorimeter (Model: Q20, TA Instrument, Inc., New Castle, DE, USA) was used to record the thermal behaviors of pure ACV, pure glucosamine HCl, the physical mixture (PM, 1:3) of pure ACV and glucosamine HCl, and the prepared ACV-SD. Thermograms of these samples were compared and analyzed. Individual samples (~ 2 mg) were press-sealed in aluminum pans and analyzed on the equipment previously calibrated with an indium standard. Each sample was subjected to a heating cycle from 0°C to 400°C at a ramp rate of 10°C/min, under a continuous purge of nitrogen (50 mL/min). The universal analysis software (Version 4.5A, build 4.5.0.5, TA Instruments, Inc., New Castle, DE, USA) accompanied by the instrument was used to analyze and interpret the obtained thermograms.

Fourier transforms infrared spectroscopy (FTIR)

Pure ACV, glucosamine HCl, PM, and ACV-SD samples were subjected to FTIR analysis in an attempt to understand their chemical differences as well as any interactions between the ACV and glucosamine HCl, either in a physical mixture or within the prepared dispersion. The spectra were collected using an FTIR spectrophotometer (Model: FTIR-8300, Shimadzu, Kyoto, Japan) following the procedure reported by Telange *et. al.* (30), and compared in order to identify the occurrence of any intermolecular interactions.

Powder x-ray diffractometry (PXRD)

The crystal characteristics of the drug, the carrier, their physical mixture (1:3), and the prepared solid dispersion were investigated by PXRD. The diffractograms were obtained on a bench-top x-ray diffractometer (MODEL: D8 ADVANCE, Bruker AXS, Inc., Madison, WI, USA), using the method reported previously by Telange *et. al.* (29).

Estimation of ACV content in ACV-SD

The ACV content in the prepared ACV-SD was estimated spectrophotometrically, following a procedure described by Chaudhary *et. al.* (31). The appropriate quantity of ACV-SD powder (containing ~100 mg ACV) was dissolved in 100 mL phosphate buffer (0.05 M, pH 6.8). The resulting solution was filtered (membrane filter, 0.45 μm), and after relevant sequential dilutions, analyzed using a UV-visible spectrophotometer (MODEL: V-630, JASCO International Co., Ltd., Tokyo, Japan) at 251 nm. The sample absorbance values were compared against those from a blank (a solution of glucosamine HCl in phosphate buffer) to calculate the amount of free ACV in the ACV-SD. The ACV content (%) incorporated in the prepared SD formulations was calculated using Equation 1.

$$\text{ACV content}(\%) = \frac{\text{total ACV (mg)} - \text{free drug (mg)}}{\text{total ACV (mg)}} = x\,100 \qquad \text{Eq. 1}$$

Aqueous solubility analysis

The aqueous solubilities of pure ACV, ACV in the physical mixture, and ACV in the prepared dispersions were determined using a procedure mimicking the one described by Al-Hamidi *et. al.* (27). Excess amounts of samples were individually dispersed in 10 mL distilled water in screw-cap glass vials and agitated on a rotary shaker (Model: RS-24 BL, REMI Laboratory Instruments, Remi House, Mumbai, India) at 37°C for 24 hours. The dispersions were then filtered (0.45 μm), diluted, and the absorbance of the resulting solutions was measured on a UV-visible spectrophotometer (MODEL: V-630, JASCO International Co., Ltd., Tokyo, Japan) at 251 nm. The absorbance values, after comparison with a blank and a standard solution of ACV, were used to calculate the aqueous solubility of ACV.

Functional characterization of ACV-SD

In vitro dissolution studies

Comparative assessment of the release pattern of pure ACV and ACV from ACV-SD was performed using a USP Type II (paddle) dissolution equipment (Model: TDT-08LX, Electrolab India Pvt. Ltd., Mumbai, India). Each dissolution run was conducted by dispersing pure ACV (40 mg) or ACV-SD (~40 mg ACV) in the dissolution vessel containing freshly

prepared phosphate buffer (900 mL, 0.05 N, pH 6.8) maintained at 37°C. The experiment was carried out for 120 minutes at 100 RPM stirring speed. Sample aliquots for testing were collected at 10 minute intervals and replaced with equal volumes of fresh medium. The test samples, after filtration and appropriate dilutions, were measured for absorbance using a UV-visible spectrophotometer (MODEL: V-630, JASCO International Co., Ltd., Tokyo, Japan) at 251 nm. The absorbance values, after comparison with a blank and a standard solution of ACV, were used to calculate the cumulative dissolution profiles of ACV and ACV-SD.

Influence of fasted *versus* fed-state media

The influence of fasted *versus* fed state on the dissolution behavior of pure ACV and ACV-SD was assessed by conducting dissolution tests using standard Fasted (FaSSIF) and Fed-state (FeSSIF) dissolution media. The media were prepared using the procedure reported by Klein *et. al.* (32). The dissolution was performed on a USP Type II (paddle) dissolution test apparatus (Model: TDT-08LX, Electrolab India Pvt. Ltd., Mumbai, India). Each dissolution run was conducted by dispersing pure ACV (100 mg) or ACV-SD (~100 mg ACV) in the dissolution vessel containing either FaSSIF (500 mL) or FeSSIF (1000 mL) maintained at 37°C. The dissolution was carried out for 120 min at a paddle stirring speed of 50 RPM. Aliquots of samples were collected at 10 minute intervals for testing and replaced with an equal volume of the blank medium. The test samples, after filtration and appropriate dilutions, were measured for absorbance on a UV-visible spectrophotometer (Model: V-630, JASCO International Co., Ltd., Tokyo, Japan) at 248.2 nm (FaSSIF) or 272 nm (FeSSIF). The absorbance values were used to calculate the cumulative dissolution profiles of ACV and ACV-SD in respective media.

Permeability across a biological membrane

The biological permeability of pure ACV and ACV in the prepared dispersion was assessed using the everted rat intestine method previously reported by Dixit *et. al.* (33). The details of the method, including the design and assembly of the apparatus, the use of experimental animals, and so on has been reported previously and followed as described therein (34). Briefly, the isolated intestinal membrane was mounted on the apparatus filled with Krebs solution (250 mL) as a permeation medium. The test sample solutions i.e., pure ACV (100 μg/mL) or ACV-SD (~100 μg/mL), prepared using Krebs solution, were placed in the apparatus on the mucosal side of the membrane. The medium was maintained at 37°C and continuously stirred at 25 RPM for a period of 120 minutes. Aliquots of samples were withdrawn at regular intervals from the serosal side of the membrane, and after filtration and appropriate dilutions, were measured for absorbance using a UV-visible spectrophotometer (MODEL: V-630, JASCO International Co., Ltd., Tokyo, Japan) at 250.4 nm. The obtained absorbance values were used to calculate the cumulative permeability profiles of ACV and ACV-SD.

Preliminary stability assessment

The optimized ACV-SD formulation i.e., ACV-SD3 was evaluated for its functional stability upon storage under controlled storage conditions (25°C at 60% RH). The samples were packaged in screw-capped, high-density polyethylene (HDPE), amber-colored bottles, and stored in an environmental chamber (Model: TS00002009, Mumbai, Maharashtra, India) for a period of six months. At the end of six months, the samples were retrieved and subjected to dissolution and permeability studies using the respective procedures described above.

Statistical analysis

The results are presented as mean ± standard deviation. The statistical analysis for comparing differences between test samples was performed using a one-way analysis of variance (ANOVA) followed by a Dunnett's or a Students t-test. P values of ≤ 0.05 were considered as a statistically significant difference.

RESULTS AND DISCUSSION

Physical-chemical characterization of ACV-SD

Photomicroscopy and scanning electron microscopy (SEM)

Microscopic images of pure ACV, pure glucosamine HCl, and ACV-SD, captured at 20X magnification are shown in Figure 1 (A, B, and C). Pure ACV (Figure 1A) appeared as small, regular crystals with well-defined geometric faces and edges. The morphology of these crystals appeared to correspond to the monoclinic polymorphic form V of ACV (35). The glucosamine HCl particles (Figure 1B) appeared to be relatively larger, globular particles with a smooth surface. The particles of ACV-SD (Figure 1C) appeared as non-uniform, clusters with ill-defined morphology. The defining characteristics of pure ACV or pure glucosamine HCl were absent in ACV-SD.

Further analysis of these particles using SEM imaging confirmed the observations from the photo-microscopic images (Figure 1a, 1b, and 1c). Pure ACV exhibited a crystalline, regular structure with geometric angles (Figure 1a). Pure glucosamine HCL showed larger particles with a rounded, smooth surface. The ACV-SD particles appeared as irregular clusters/ aggregates formed as a result of the physical interaction between ACV and glucosamine HCl.

Particle size and zeta potential analysis

The mean particle size and zeta potential are considered relevant markers indicative of the physical stability of sub-micron particles dispersed in a liquid medium (29). Particles sizes $\leq$ 500 nm are known to prefer endocytosis as a major pathway of transport across biological membranes (36). The mean particle size of the prepared ACV-SD was ~120 nm with a polydispersity index (PDI) of 31.06 (Figure 2A). The

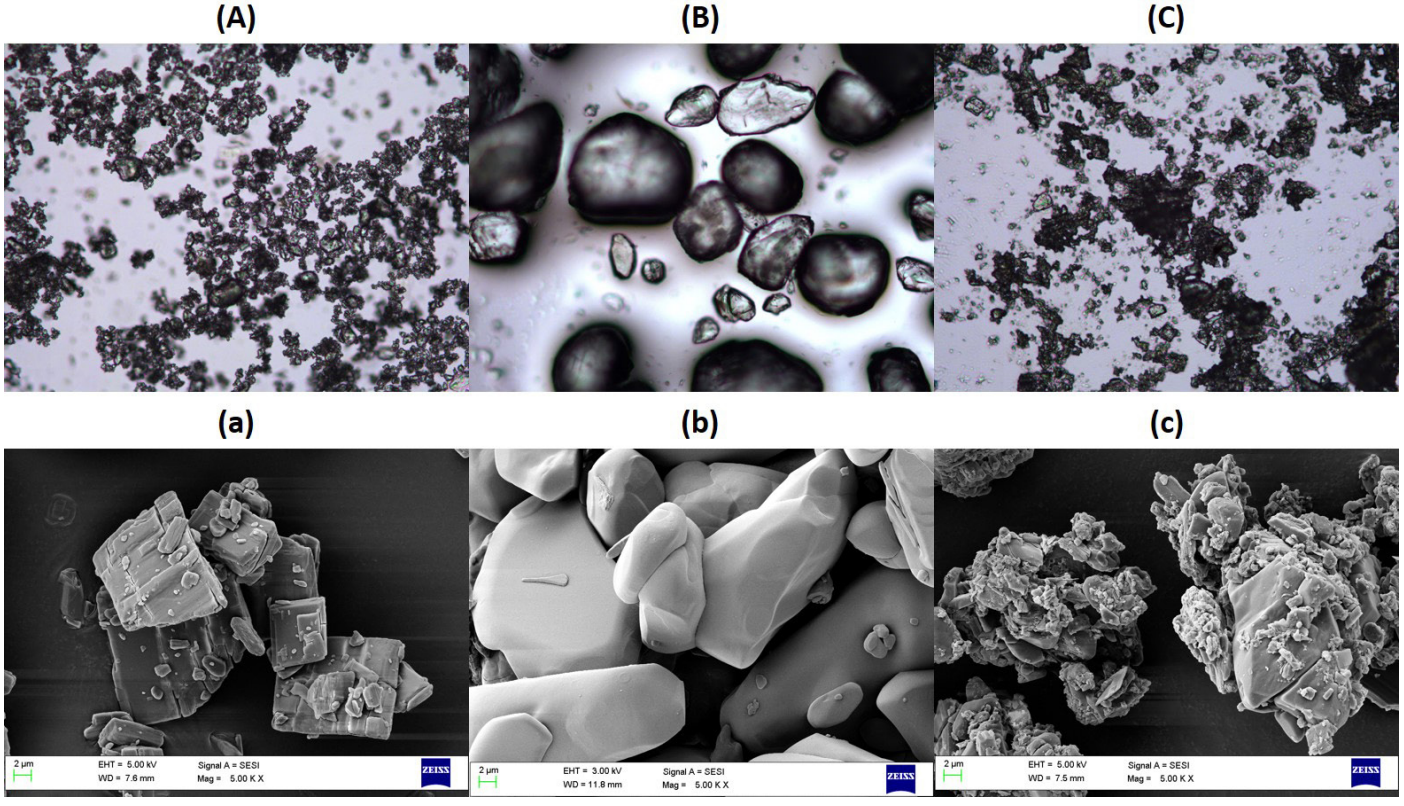

Figure 1 Photomicroscopy images of (A) pure acyclovir, (B) pure glucosamine HCl, and (C) acyclovir-glucosamine HCl solid dispersion. Scanning electron microscopy images of (a) pure acyclovir, (b) pure glucosamine HCl, and (c) acyclovir-glucosamine HCl solid dispersion (ACV-SD).

prepared formulation thus has a sub-micron particle size and a narrow distribution.

Zeta potential (ζ) often indicates the relative physical stability of multiparticulate, disperse systems. The measured zeta potential value of the prepared ACV-SD formulation was – 39.43 ± 0.23 mV (Figure 2B), indicating that the prepared formulation dispersion is relatively stable, and bereft of any aggregation potential (28).

Thermal analysis

Physical interactions, if any, between the components of a formulation, are generally quite conveniently assessed using comparative thermal analysis. Such interactions are generally revealed in the form of appearance, disappearance, shifting, or changes

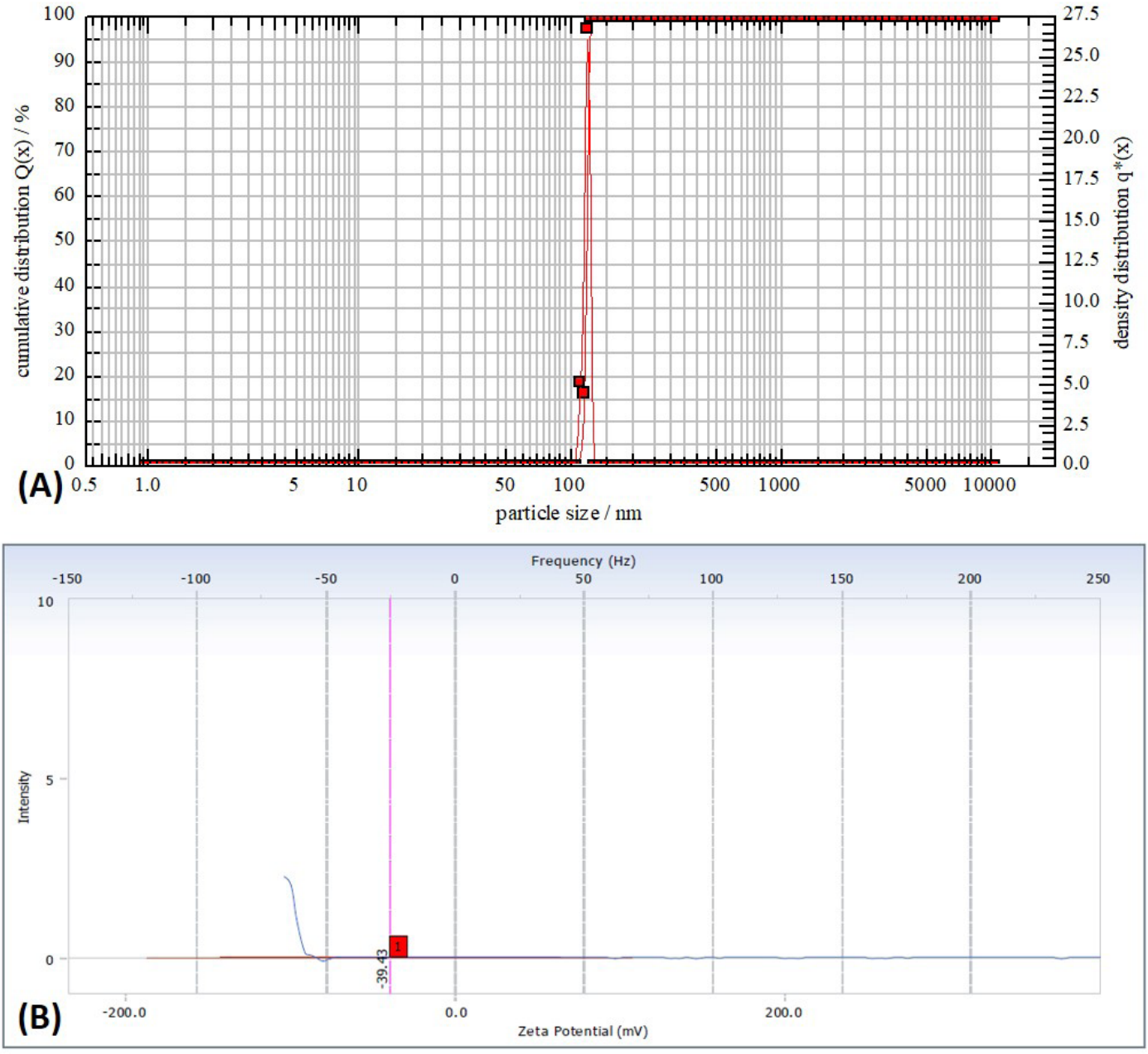

Figure 2 Particle size distribution (A) and zeta potential (B) of the prepared ACV-SD formulation.

in the onset and/or relative areas of the peaks as a function of controlled temperature increases. These interactions may indicate melting, degradation, and/or incompatibilities between the components of the formulation.

Figure 3 (A, B, C, and D) shows the thermograms obtained from the DSC analysis of pure ACV, pure glucosamine HCl, the physical mixture (PM, 1:3) of pure ACV and glucosamine HCl, and the prepared ACV-SD. The thermogram of pure ACV (Figure 3A) exhibited a sharp peak at ~256°C, indicative of the melting temperature of ACV. Another minor endothermic event was observed for pure ACV between ~60°C and ~ 175°C (not apparent in the figure). This event may be attributed to the phase transition of polymorphic hydrate form V to anhydrous form III in the range of 65°C and 100°C, and thereafter from form III to anhydrous form VI at higher temperatures. These changes in the thermal characteristics of ACV are not uncommon and have been reported earlier (9, 10, 37). The thermogram of glucosamine HCl (Figure 3B) revealed two, broad, fused endothermic peaks; a larger peak with an onset at ~190°C and a smaller peak

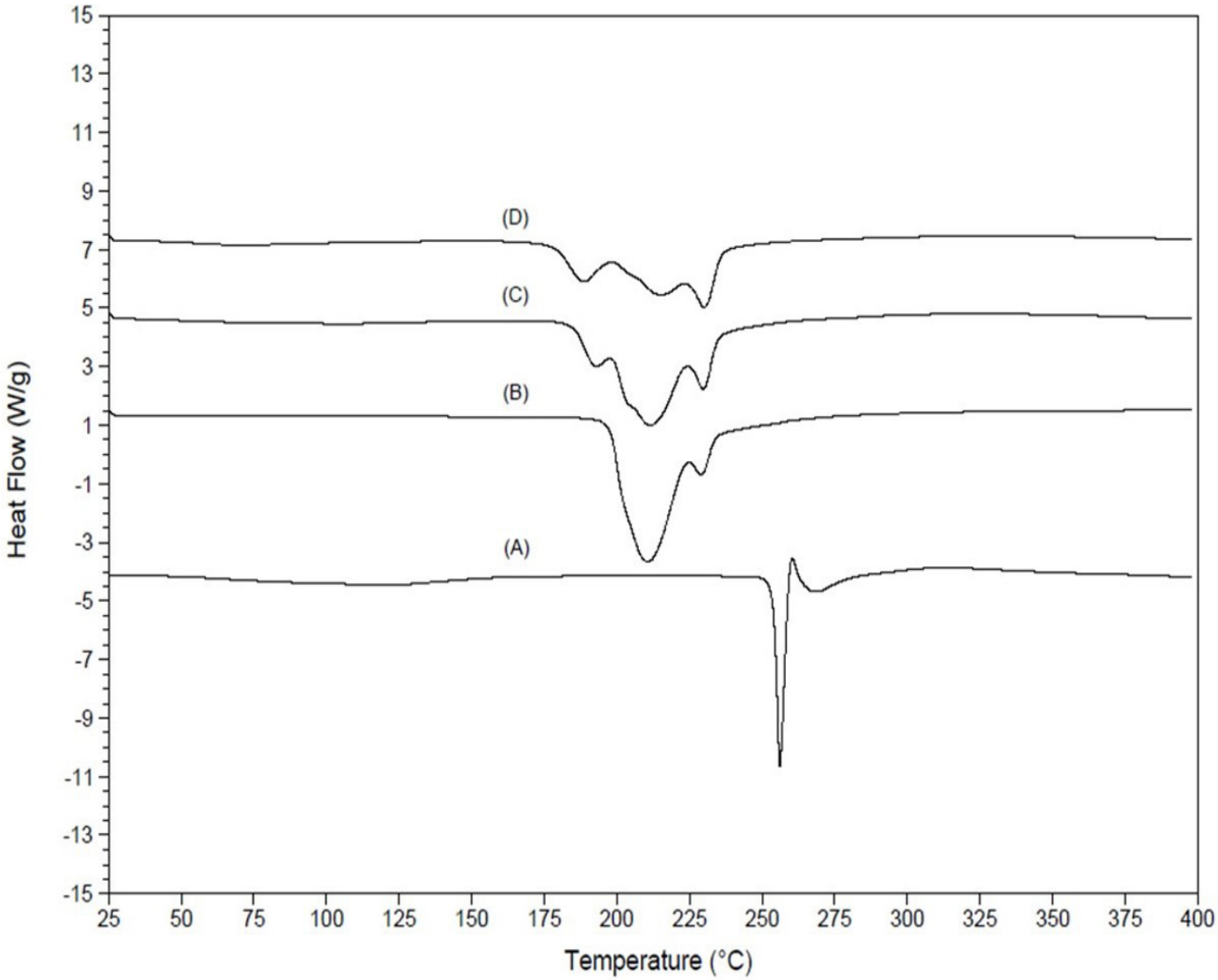

Figure 3 DSC thermograms of (A) pure ACV, (B) pure glucosamine HCl, (C) the physical mixture (1:3) of ACV and glucosamine HCl, and (D) the prepared ACV-SD formulation.

at ~229°C. The first peak is likely associated with the melting of glucosamine HCl, and the second, smaller peak may be associated with its degradation. These results are in agreement with previously published reports (26, 27). The thermograms of the physical mixture (Figure 3C) exhibited broad, fused peaks similar to that of pure glucosamine HCl, along with the disappearance of the melting peak of ACV. It is likely that with increasing temperatures, glucosamine HCl melted earlier at around 190°C and ACV dispersed/dissolved in the carrier matrix in situ. The thermogram of ACV-SD (Figure 3D) revealed broad, diffused endothermic peaks that were uncharacteristic of either pure ACV or pure glucosamine HCl. The absence of defining peaks of ACV and glucosamine HCl in ACV-SD thermogram is expected to owe the possibility that ACV is molecularly dispersed into the carrier matrix, resulting in partial amorphization of ACV.

Fourier transform infrared spectroscopy (FTIR)

The spectra obtained from the infrared analysis of pure ACV, pure glucosamine HCl, the physical mixture (PM, 1:3) of pure ACV and glucosamine HCl, and the prepared ACV-SD are shown in Figure 4A, 4B, 4C, and 4D, respectively. For pure ACV (Figure 4A), characteristic absorption bands were located at ~3622 cm-1 (primary amine) and 3411 cm^{-1} (secondary amine, N-H stretching). Additional peaks typically associated with ACV were found at ~1712 cm^{-1} (C=O stretching), ~1630 cm^{-1} and ~1609 cm^{-1} (amine), ~1483 cm^{-1} (O-H stretching), and ~1347 cm^{-1} (C-H stretching). These observations were consistent with previous findings (10, 38). The FTIR spectrum of glucosamine HCl (Figure 4B) exhibited a characteristic absorption peak at ~3291 cm^{-1} (N-H and O-H stretching). Other peaks related to glucosamine were observed at ~3000 cm^{-1} and 2881 cm^{-1} (-C-H stretching), ~1618 cm^{-1} and 1537 cm^{-1} (N-H bending), ~1140 cm^{-1} (asymmetric

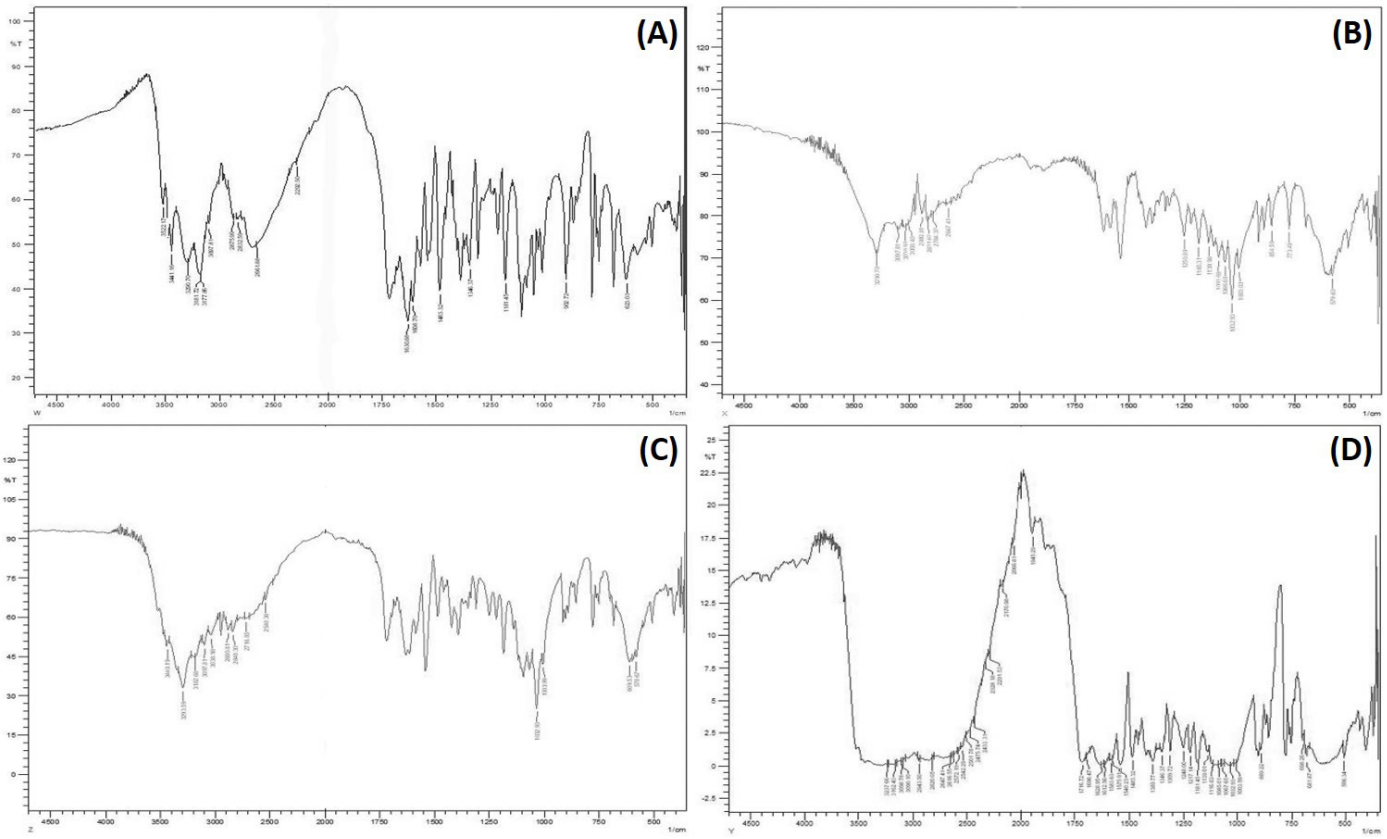

Figure 4 FTIR spectra of (A) pure ACV, (B) pure glucosamine HCl, (C) the physical mixture (1:3) of ACV and glucosamine HCl, and (D) the prepared ACV-SD formulation.

C-O-C stretching) and ~1094 cm^{-1} (C-O functional group). These results were analogous to those reported earlier (39). The spectrum of the physical mixture of the drug and the carrier (Figure 4C) showed peaks corresponding mostly to glucosamine HCl, albeit with higher absorbance intensities. The higher ratio of glucosamine HCl in the mixture can be attributed to the observed predominance of glucosamine related peaks. The FTIR plot of ACV-SD formulation (Figure 4D) was found to be significantly different compared to those of the individual components. The characteristic peaks associated with pure ACV and pure glucosamine HCl were absent in this spectrum. Several absorption peaks were observed in the region between 3300 cm^{-1} and 1085 cm^{-1}. The presence of unique peaks in this spectrum can be likely attributed to hydrogen bonding between the N-H functional group of ACV and the O-H group of glucosamine HCl, and the formation of solid dispersion (10, 27). The formation of solid dispersion not only helps in solubilizing the API into the hydrophilic carrier but also likely prevents the recrystallization of the drug in the glass solution (40).

Powder x-ray diffractometry (PXRD)

Powder x-ray diffractometry (PXRD) provides useful information on the crystalline properties and any polymorphic changes in the components of a formulation. The diffractograms obtained from the PXRD analysis of pure ACV, pure glucosamine HCl, the physical mixture (PM, 1:3) of pure ACV and glucosamine HCl, and the prepared ACV-SD are shown in Figure 5 (A, B, C and D). The diffractogram of pure ACV (Figure 5A) showed a sharp, high-intensity peak at ~7° 2θ, related to ACV crystal structure. Other low-intensity peaks were observed at ~ 10.5°, 21°, 26°, and 29° on the 2θ scale. All these peaks are associated with the polymorphic form V of ACV and in agreement with earlier published reports (10). The diffraction pattern

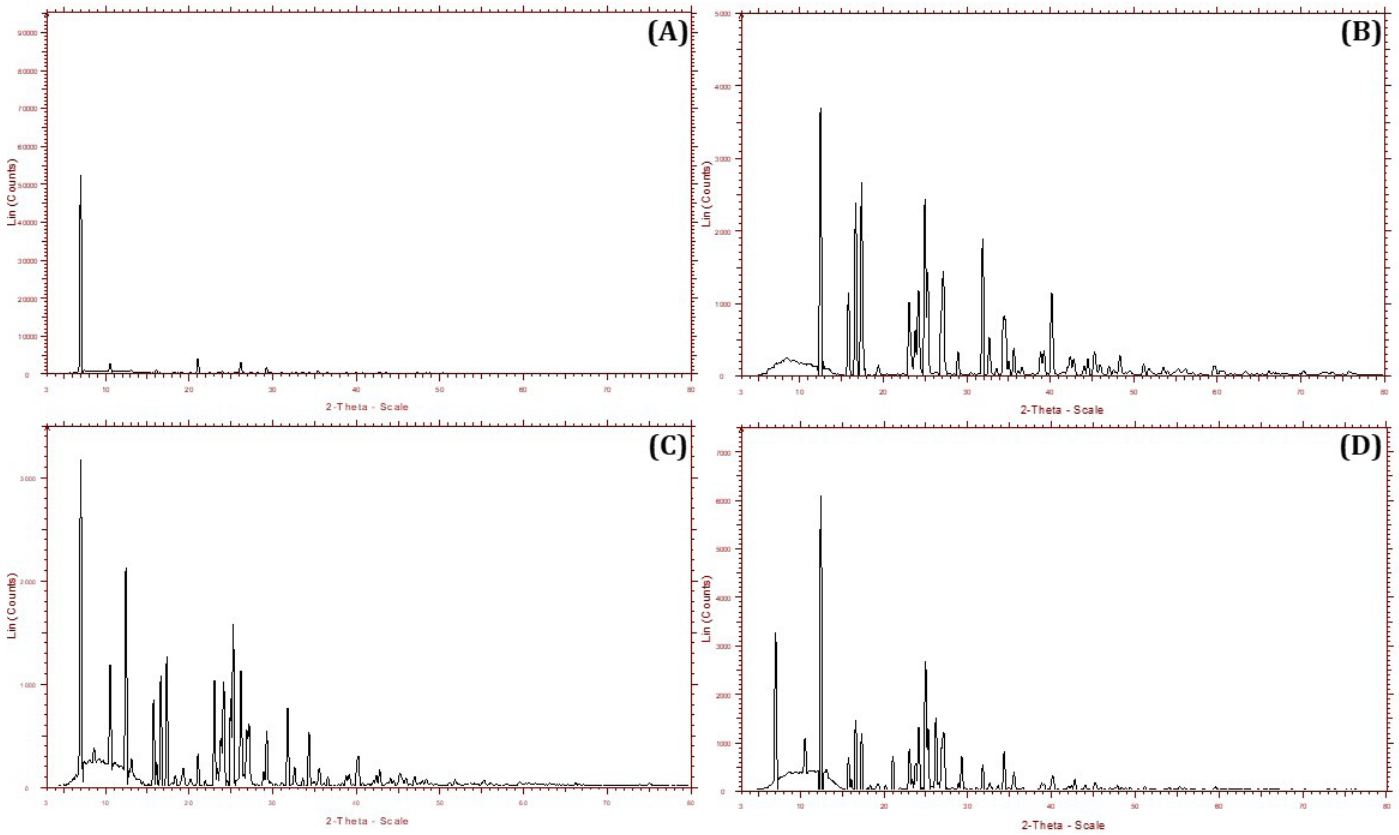

Figure 5 The x-ray diffractograms of (A) pure ACV, (B) pure glucosamine HCl, (C) the physical mixture (1:3) of ACV and glucosamine HCl, and (D) the prepared ACV-SD formulation.

of glucosamine HCl (Figure 5B) exhibited several low and high-intensity peaks in the region between 12° 2θ and 60° 2θ, along with a partial amorphous 'halo' pattern between 5° 2θ and 15° 2θ, indicating a mostly crystalline nature of the carrier. The diffractogram was similar to that reported previously in the literature (26). The diffractogram of the physical mixture (Figure 5C) showed a series of peaks between 7° 2θ and 43° 2θ. These peaks appeared to those observed with pure ACV and pure glucosamine HCl, albeit with lower intensities for peaks associated with ACV. Finally, the diffractogram of ACV-SD revealed peaks that were of significantly lower in number and intensities compared to the pure components (Figure 5D). The diffractogram appeared to retain the characteristic peaks of the carrier, whereas, ACV-related peaks were greatly minimized. It is likely that ACV is partially amorphized in the prepared solid dispersion.

Estimation of the ACV content in ACV-SD

The ACV content in the prepared ACV-SD is represented as % ACV incorporated in Table 2. For all ACV-SD formulations, the ACV content was found to be > 95% w/w. The formulation ACV-SD3 (drug-carrier ratio of 1:3) showed the highest incorporation efficiency (98.17 ± 0.49 %) and was used as an optimal formulation for most of the characterization studies. The high incorporation efficiency of ACV in the prepared formulation supported the selection of carrier and the robustness of the formulation approach.

Aqueous solubility analysis

The results obtained from the aqueous solubility analysis of pure ACV, the physical mixtures of ACV and glucosamine HCl, and the prepared ACV-SD formulations are presented in Table 3. Pure ACV exhibited aqueous solubility of ~14 μg/mL. This is not surprising, as ACV is a known BCS Class III (↑ solubility, ↓ permeability) or class IV (↓ solubility, ↓ permeability) drug (18). The results are in agreement with previously published aqueous solubility values for ACV (9, 41). The solubilities of ACV in the physical mixtures ranged between 82 and 85 μg/mL. These values represented a nearly 6-fold higher solubility of ACV in the physical mixture compared to that of ACV alone. A close association of the water-soluble carrier resulting in an increased wetting efficiency of ACV particles in the aqueous medium is a likely cause for the observed higher aqueous solubility of ACV in the physical mixture. Among the physical mixtures, ACV-SD3 (drug-carrier ratio of 1:3) exhibited the highest observed solubility of ACV. Further increase in the ratio of carrier probably restricted ACV particles access to water, resulting in the observed modest decrease in ACV solubility (27). The prepared ACV-SD formulations exhibited significantly higher solubilities of ACV, compared to that of pure ACV or ACV in the physical mixtures. The solubilities of ACV in these formulations ranged between 165 and 191 μg/mL. These results represented a nearly 12-fold increase in the solubility of ACV compared to that of ACV alone,

Table 2 Drug content of acyclovir in prepared solid-dispersion formulations

FORMULATION	DRUG CONTENT (%, w/w)*
ACV-SD1	95.30 ± 0.65
ACV-SD2	97.21 ± 1.32
ACV-SD3	98.17 ± 0.49
ACV-SD4	96.10 ± 1.01
ACV-SD5	96.44 ± 1.20

*All results are expressed as mean ± Std. Dev., n=3

Table 3 Aqueous solubility of pure acyclovir, acyclovir in physical mixture (PM), and acyclovir in the prepared solid-dispersions

FORMULATION	AQUEOUS SOLUBILITY (μg/mL)*
Pure acyclovir	13.91 ± 0.02
PM-1	82.25 ± 0.03
PM-2	84.59 ± 0.02
PM-3	85.11 ± 0.08
PM-4	83.27 ± 0.04
PM-5	84.40 ± 0.03
ACV-SD1	165.15 ± 0.02
ACV-SD2	171.28 ± 0.08
ACV-SD3	191.33 ± 0.06
ACV-SD4	183.49 ± 0.06
ACV-SD5	180.36 ± 0.07

*All results are expressed as mean ± Std. Dev., n=3

and a 2-fold increase compared to that of ACV in the physical mixture. The solubilities of ACV within these formulations followed a trend similar to that observed with the physical mixtures. The observed enhanced aqueous solubility of ACV in these formulations may be attributed to carrier-assisted modifications of the physical-chemical properties of ACV such as changes in the particle size, morphology, and polymorphic state (26).

Functional characterization of ACV-SD

In vitro dissolution studies

The comparative dissolution profiles of pure ACV and the ACV-SD formulations prepared using different drug-carrier ratios, in phosphate buffer (0.05 M, pH 6.8) are represented in Figure 6. Pure ACV exhibited an initial rapid dissolution (~30% in 10 minutes), followed by a steady, zero-order release over a period of 2 hours. At the end of the dissolution period, the extent of cumulative ACV dissolution was recorded at ~62%. The relatively lower dissolution efficiency of pure ACV is attributable to its low aqueous solubility. The rate and extent of ACV dissolution from the prepared ACV-SD formulations followed the trend observed with the solubility studies, i.e., cumulative rate and extent of ACV dissolution increased in formulations with increasing drug-carrier ratio, up to the ratio of 1:3. For formulations with a drug-carrier ratio of 1:4 and 1:5 the cumulative dissolution of ACV was observed to be relatively slower and to a lesser extent. This is possibly due to the higher concentration of carrier inhibiting the access of ACV particles to the dissolution media (27). ACV-SD3 (drug-carrier ratio of 1:3) exhibited the highest observed rate and extent of ACV dissolution (~94%). Earlier studies suggested that solvent-evaporation-method-based solid dispersions produce high energy solid-state formulations by partial amorphization of drug particles, which increases the dissolution rate of drugs (17). Another possibility for explaining enhanced aqueous solubility may be the hydrophilic nature of glucosamine HCl increasing the

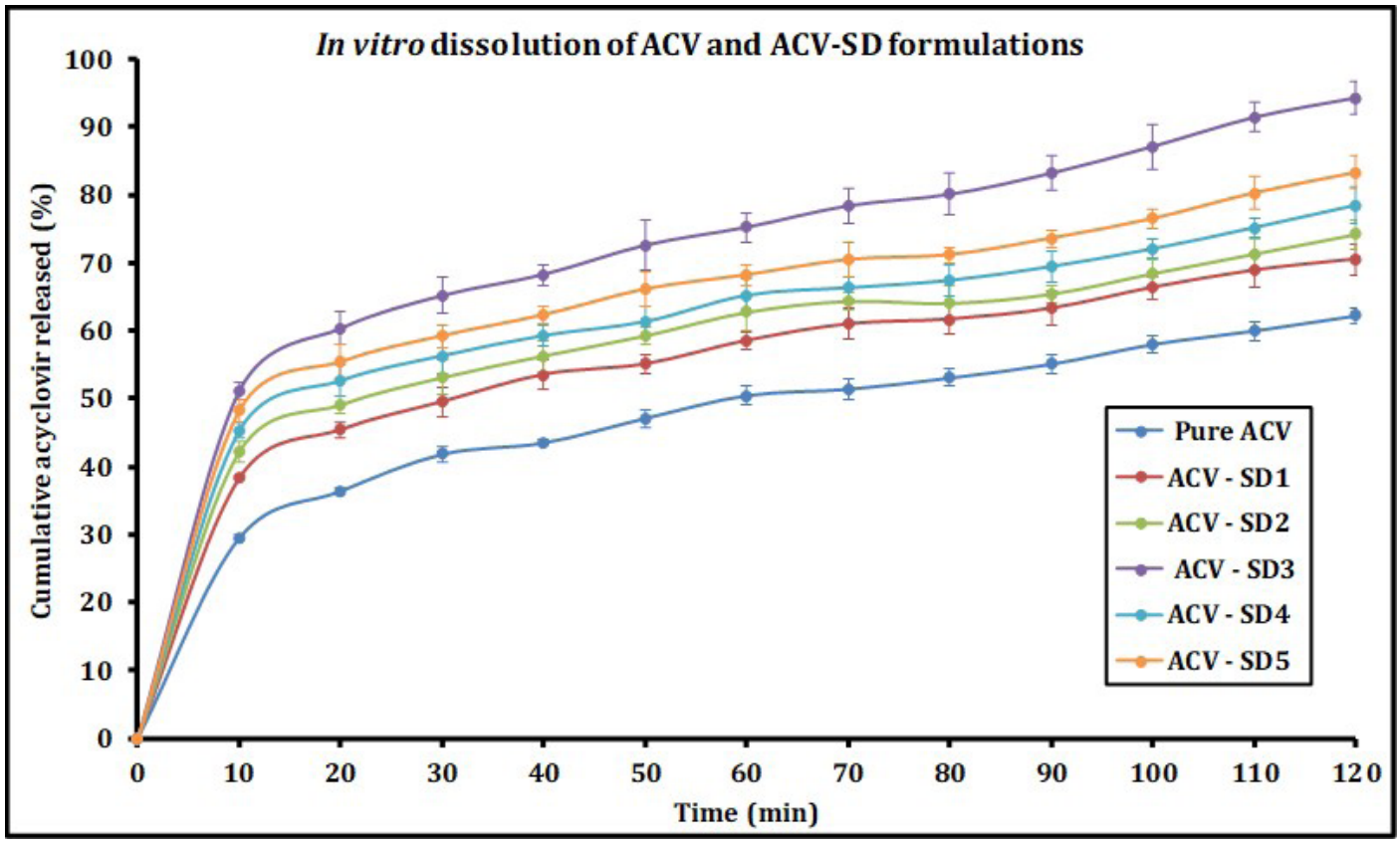

Figure 6 The comparative *in vitro* dissolution profiles of ACV and ACV-SD3 formulations.

wettability of dispersed ACV particles in ACV-SD (26).

Influence of fasted versus fed state media

Figure 7 shows a comparison of the dissolution profiles of pure ACV and that of ACV from ACV-SD3 formulation as tested in FaSSIF (fasted) and FeSSIF (fed) media. The efficiency of the dissolution of pure ACV was found to be lower in fasted conditions compared to that in fed conditions. At the end of the 2-hour dissolution period, only about 43% of pure ACV had dissolved. In fed conditions, there was a modest, albeit significant increase in the efficiency of ACV dissolution (~64% at the end of 2 hours). Positive food effects on the dissolution of drugs with low aqueous solubility have been reported earlier (32, 42). The rate and extent of ACV release from ACV-SD3 were found to be higher in both fasted and fed conditions compared to that of pure ACV. In fasted conditions ~76%, and in fed conditions ~84% ACV was released at the end of the 2-hour dissolution period. These results correlated well with those obtained from the solubility analysis and the in vitro dissolution studies.

Permeability across a biological membrane

The comparative permeabilities of pure ACV and ACV-SD formulations across a biological membrane, as evaluated by the everted rat intestine model are shown in Figure 8. After the 2-hour testing period, only about 42% of pure ACV had permeated across the membrane. ACV is reported at a BCS class III or IV drug (low permeability), and thus the results are consistent with those published previously (8, 18). The permeability profiles of ACV from all ACV-SD formulations were found to be relatively higher compared to that of pure ACV. The permeability of ACV from these formulations followed the trend observed with the results obtained from solubility and dissolution studies. In general, the rate and extent of ACV permeability increased with increasing

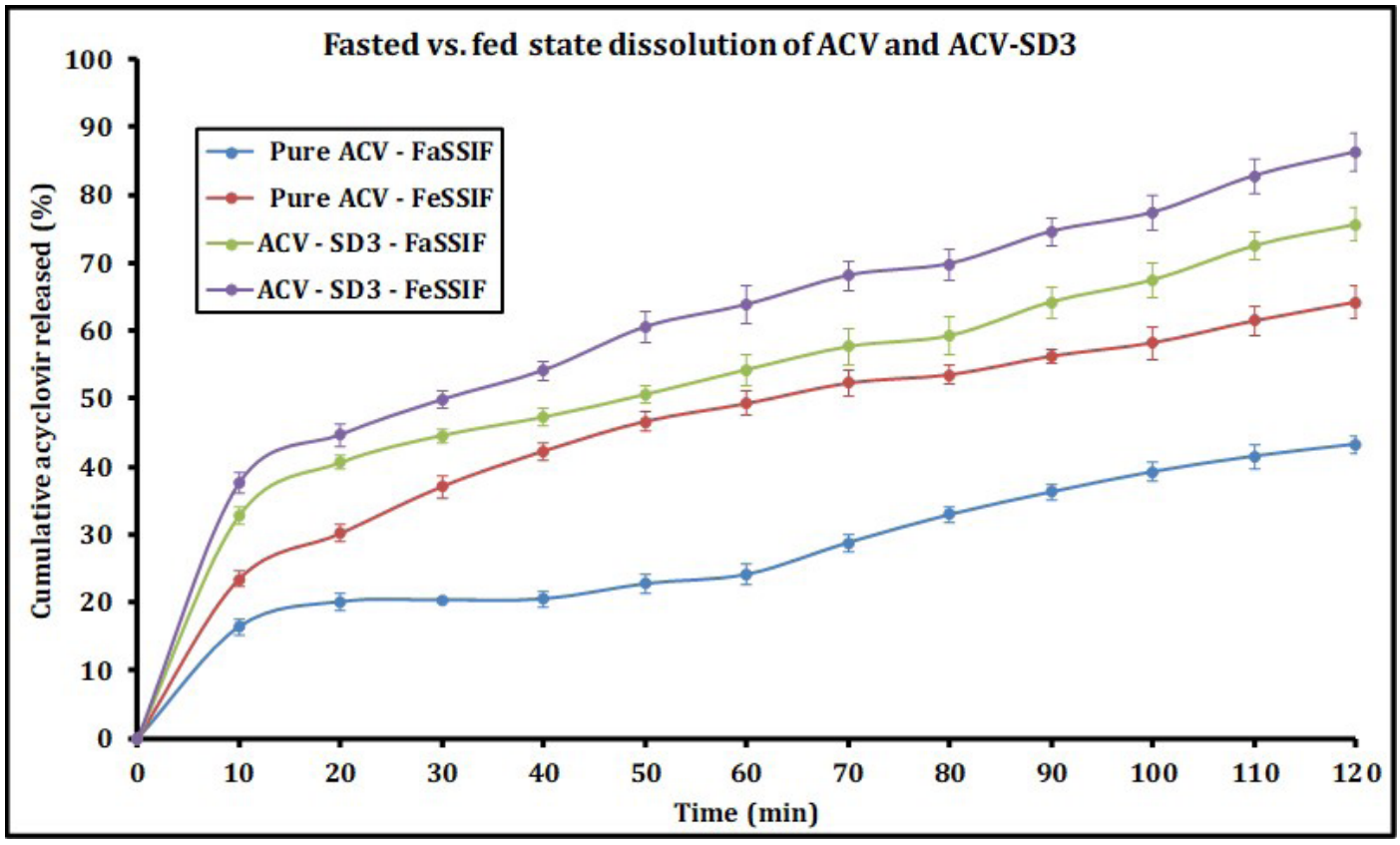

Figure 7 The influence of fasted and fed-state conditions on the dissolution behavior of pure ACV and the ACV-SD formulations.

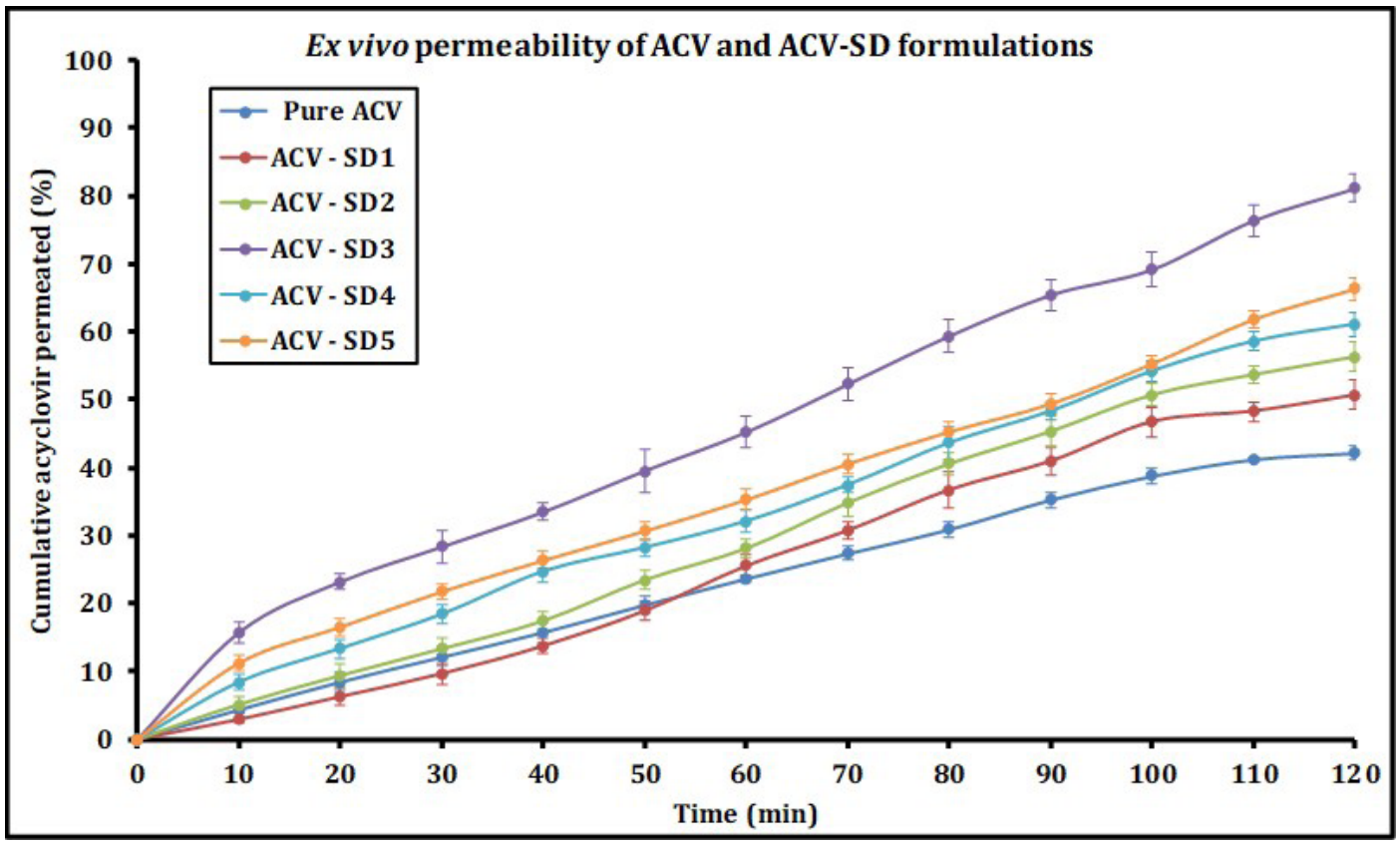

Figure 8 The comparative ex vivo permeability profiles of the ACV and ACV-SD formulations.

drug-polymer ratio up to 1:3. ACV permeability was observed to be lower for formulations with a drug-carrier ratio of 1:4 and 1:5. ACV-SD3 (drug-carrier ratio of 1:3) exhibited the highest observed efficiency of ACV permeability.

Preliminary stability assessment

The results obtained from the preliminary stability assessment of the selected ACV-SD3 formulation was stored at controlled temperature (25°C) and relative humidity (60 ± 5% RH) for 6 months are shown in Figure 9. Figure 9A shows a comparison of dissolution profiles of ACV-SD3 at day 0 and day 180 (6 months). It was observed that while the drug release from the 180-day sample followed a pattern similar to that of day 0 sample, there was a noticeable decrease in the efficiency of ACV dissolution at the end of the duration of the study. Figure 9B compares the permeability profiles of ACV-SD3 at day 0 and day 180. Similar to the dissolution results, there was a noticeable decrease in the efficiency of ACV permeability for the samples stored for 180 days, whilst the permeability profile followed matching patterns. The reasons for this shift in the dissolution and permeability of ACV-SD are currently unclear. It is possible that the storage conditions, mainly the relative humidity have had an influence on the physical-chemical properties of ACV or the solid dispersion. Further characterization of the stored samples is currently underway.

CONCLUSIONS

The present study aimed to study the feasibility of utilizing a relatively unexplored, hydrophilic excipient, glucosamine HCl as a solid-dispersion carrier with the goal of enhancing the biopharmaceutical properties of drugs with low aqueous solubility. Solid dispersion based formulations of acyclovir combined with glucosamine HCl were successfully prepared using a previously established solvent-evaporation method. The prepared formulations were characterized for

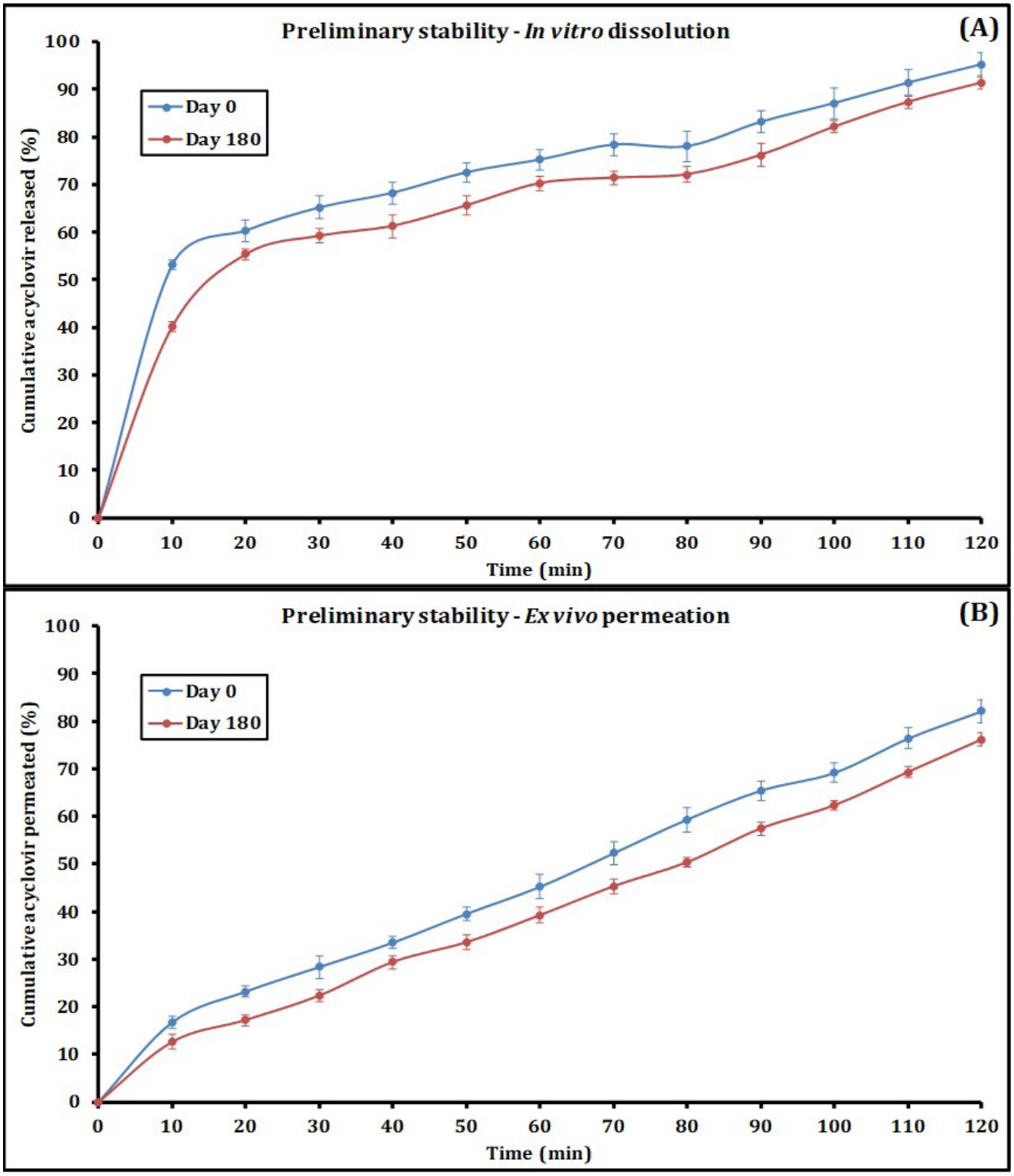

Figure 9 The effect of controlled storage conditions (25°C/60% RH, 180 days) on (A) dissolution and (B) permeability of ACV-SD3.

their physical and functional properties using various analytical methods. The prepared ACV-glucosamine HCl solid dispersions demonstrated marked increases in aqueous solubility, dissolution, and permeability of acyclovir compared to the pure drug. The prepared solid dispersions were not found to be drastically unstable, the storage conditions appeared to have a modest influence on the physical-chemical properties of either the drug or the formulation. While the nature of this influence is unclear, further characterization of the stored samples is warranted. The study overall demonstrates the feasibility of utilizing glucosamine HCl as a potential solid-dispersion carrier to improve the biopharmaceutical properties of drugs with low solubility and/permeability characteristics.

REFERENCES

1 Shukla, D., et al., Lipid-based oral multiparticulate formulations - advantages, technological advances and industrial applications. Expert Opin. Drug Deliv., 2011. 8(2): p. 207-24.

2 Svenson, S., Dendrimers as versatile platform in drug delivery applications. Eur. J. Pharm. Biopharm., 2009. 71 (3): p. 445-62.

3 Kawabata, Y., et al., Formulation design for poorly water-soluble drugs based on biopharmaceutics classification system: Basic approaches and practical applications. Int. J. Pharm., 2011. 420 (1): p. 1-10.

4 Yu, L.X., et. al., Biopharmaceutics classification system: the scientific basis for biowaiver extensions. Pharm. Res., 2002. 19 (7): p. 921-5.

5 Rinaki, E., G. Valsami, and P. Macheras, Quantitative Biopharmaceutics Classification System: The Central Role of Dose/Solubility Ratio. Pharm. Res., 2003. 20 (12): p. 1917-1925.

6 Alsarra, I.A., A.Y. Hamed, and F.K. Alanazi, Acyclovir Liposomes for Intranasal Systemic Delivery: Development and Pharmacokinetics Evaluation. Drug Delivery, 2008. 15 (5): p. 313-321.

7 Kharia, A.A. and A.K. Singhai, Development and optimisation of mucoadhesive nanoparticles of acyclovir using design of experiments approach. J. Microencapsul., 2015. 32 (6): p. 521-32.

8 Moniruzzaman, M., et. al., Ionic liquid-in-oil microemulsion as a potential carrier of sparingly soluble drug: Characterization and cytotoxicity evaluation. Int. J. Pharm., 2010. 400 (1): p. 243-250.

9 Nair, A.B., et. al., Enhanced oral bioavailability of acyclovir by inclusion complex using hydroxypropyl-β-cyclodextrin. Drug Delivery, 2014. 21 (7): p. 540-547.

10 Nart, V., et. al., Ball-milled solid dispersions of BCS Class IV drugs: Impact on the dissolution rate and intestinal permeability of acyclovir. Materials Science and Engineering: C, 2015. 53: p. 229-238.

11 Rarokar, N.R., S.D. Saoji, and P.B. Khedekar, Investigation of effectiveness of some extensively used polymers on thermoreversible properties of Pluronic® tri-block copolymers. Journal of Drug Delivery Science and Technology, 2018. 44: p. 220-230.

12 Rarokar, N.R., et. al., Nanostructured Cubosomes in a Thermoresponsive Depot System: An Alternative Approach for the Controlled Delivery of Docetaxel. AAPS PharmSciTech, 2016. 17 (2): p. 436-45.

13 Shadab, et. al., Gastroretentive drug delivery system of acyclovir-loaded alginate mucoadhesive microspheres: formulation and evaluation. Drug Deliv, 2011. 18 (4): p. 255-64.

14 Valizadeh, H., et. al., Physicochemical characterization of solid dispersions of indomethacin with PEG 6000, Myrj 52, lactose, sorbitol, dextrin, and Eudragit E100. Drug Dev. Ind. Pharm., 2004. 30 (3): p. 303-17.

15 Huang, Y. and W.-G. Dai, Fundamental aspects of solid dispersion technology for poorly soluble drugs. Acta Pharmaceutica Sinica B, 2014. 4 (1): p. 18-25.

16 Serajuddin, A.T.M., Solid dispersion of poorly water soluble drugs: Early promises, subsequent problems, and recent breakthroughs. J. Pharm. Sci., 1999. 88 (10): p. 1058-1066.

17 Leuner, C. and J. Dressman, Improving drug solubility for oral delivery using solid dispersions. Eur. J. Pharm. Biopharm., 2000. 50 (1): p. 47-60.

18 Arnal, J., et. al., Biowaiver Monographs for Immediate Release Solid Oral Dosage Forms: Aciclovir. J. Pharm. Sci., 2008. 97 (12): p. 5061-5073.

19 Rottinghaus, S.T. and R.J. Whitley, Current non-AIDS antiviral chemotherapy. Expert Rev. Anti Infect. Ther., 2007. 5 (2): p. 217-30.

20 Bergström, C.A.S., et. al., Absorption Classification of Oral Drugs Based on Molecular Surface Properties. J. Med. Chem., 2003. 46 (4): p. 558-570.

21 Fletcher, C. and B. Bean, Evaluation of oral acyclovir therapy. Drug Intell. Clin. Pharm., 1985. 19 (7-8): p. 518-24.

22 Friedrichsen, G.M., et. al., Synthesis of analogs of l-valacyclovir and determination of their substrate activity for the oligopeptide transporter in Caco-2 cells. Eur. J. Pharm. Sci., 2002. 16 (1): p. 1-13.

23 Wagstaff, A.J., D. Faulds, and K.L. Goa, Aciclovir. A reappraisal of its antiviral activity, pharmacokinetic properties and therapeutic efficacy. Drugs, 1994. 47 (1): p. 153-205.

24 da Camara, C.C. and G.V. Dowless, Glucosamine sulfate for osteoarthritis. Ann. Pharmacother., 1998. 32 (5): p. 580-7.

25 Pujalte, J.M., E.P. Llavore, and F.R. Ylescupidez, Double-blind clinical evaluation of oral glucosamine sulphate in the basic treatment of osteoarthrosis. Curr. Med. Res. Opin., 1980. 7(2): p. 110-14.

26 Al-Hamidi, H., et. al., Effect of glucosamine HCl on dissolution and solid state behaviours of piroxicam upon milling. Colloids Surf. B Biointerfaces, 2013. 103: p. 189-99.

27 Al-Hamidi, H., et. al., To enhance dissolution rate of poorly water-soluble drugs: glucosamine hydrochloride as a potential carrier in solid dispersion formulations. Colloids Surf. B Biointerfaces, 2010. 76 (1): p. 170-8.

28 Dhore, P.W., et. al., Enhancement of the aqueous solubility and permeability of a poorly water soluble drug ritonavir via lyophilized milk-based solid dispersions. Pharm. Dev. Technol., 2017. 22 (1): p. 90-102.

29 Telange, D.R., et. al., Kaempferol-Phospholipid Complex: Formulation, and Evaluation of Improved Solubility, in vivo Bioavailability, and Antioxidant Potential of Kaempferol. J. Excipients and Food Chem., 2016. 7 (4): p. 89-120.

30 Telange, D.R., et. al., Drug-phospholipid complex-loaded matrix film formulation for enhanced transdermal delivery of quercetin. J. Excipients and Food Chem., 2018. 9 (2): p. 31-50.

31 Choudhary, A., et. al., Development and characterization of an atorvastatin solid dispersion formulation using skimmed milk for improved oral bioavailability. Acta Pharmaceutica Sinica B, 2012. 2(4): p. 421-428.

32 Klein, S., The use of biorelevant dissolution media to forecast the in vivo performance of a drug. The AAPS journal, 2010. 12 (3): p. 397-406.

33 Dixit, P., D.K. Jain, and J. Dumbwani, Standardization of an ex vivo method for determination of intestinal permeability of drugs using everted rat intestine apparatus. J. Pharmacol. Toxicol. Methods, 2012. 65 (1): p. 13-7.

34 Saoji, S.D., et. al., The role of phospholipid as a solubility- and permeability-enhancing excipient for the improved delivery of the bioactive phytoconstituents of Bacopa monnieri. Eur. J. Pharm. Sci., 2017. 108: p. 23-35.

35 Lutker, K.M., et. al., Polymorphs and hydrates of acyclovir. J. Pharm. Sci., 2011. 100 (3): p. 949-963.

36 Savic, R., et. al., Micellar nanocontainers distribute to defined cytoplasmic organelles. Science, 2003. 300 (5619): p. 615-8.

37 Karolewicz, B., et. al., Physicochemical characterization and dissolution studies of acyclovir solid dispersions with Pluronic F127 prepared by the kneading method. Acta Pharm, 2016. 66 (1): p. 119-28.

38 Gandhi, A., S. Jana, and K.K. Sen, In-vitro release of acyclovir loaded Eudragit RLPO((R)) nanoparticles for sustained drug delivery. Int. J. Biol. Macromol., 2014. 67: p. 478-82.

39 Veerapandian, M., et. al., Copper-Glucosamine Microcubes: Synthesis, Characterization, and C-Reactive Protein Detection. Langmuir, 2011. 27 (14): p. 8934-8942.

40 Riekes, M.K., et. al., HPMC as a potential enhancer of nimodipine biopharmaceutical properties via ball-milled solid dispersions. Carbohydr. Polym., 2014. 99: p. 474-82.

41 Liu, H., et. al., Preparation and evaluation of a novel gastric mucoadhesive sustained-release acyclovir microsphere. Drug Dev. Ind. Pharm., 2010. 36 (9): p. 1098-105.

42 Raman, S. and J.E. Polli, Prediction of positive food effect: Bioavailability enhancement of BCS class II drugs. Int. J. Pharm., 2016. 506 (1-2): p. 110-5.